Mapping of Landslides Under Dense Vegetation Cover Using Object-Oriented Analysis and LiDAR Derivatives

Miet Van Den Eeckhaut, Norman Kerle, Javier Hervás, and Robert Supper

Abstract

Light Detection and Ranging (LiDAR) and its wide range of derivative products have become a powerful tool in landslide research, particularly for landslide identification and landslide inventory mapping. In contrast to the many studies that use expert-based analysis of LiDAR derivatives to identify landslides, only few studies, all pixel-based, have attempted to develop computer-aided methods for extracting landslides from LiDAR. So far, it has not been tested whether object-oriented analysis (OOA) could be an alternative. Therefore, this study focuses on the application of OOA using LiDAR derivatives such as slope gradient, curvature, and difference in elevation (2 m resolution). More specifically, the focus is on the possible use for segmentation and classification of slow-moving landslides in densely vegetated areas, where spectral data do not allow accurate landslide inventory mapping. The test areas are the Flemish Ardennes (Belgium) and Vorarlberg (Austria). In a first phase, a relatively qualitative procedure based on expert-knowledge and basic statistical analysis was developed for a test area in the Flemish Ardennes. The procedure was then applied without further modification to a validation area in the same region. The results obtained show that OOA using LiDAR derivatives allows recognition and characterization of profound morphologic properties of deep-seated landslides, because approximately 70 % of the landslides of an expert-based inventory were also included in the object-oriented inventory. For mountain areas with bed rock outcrops like Vorarlberg, on the other hand, it is more difficult to create a transferable model.

Keywords

Deep-seated landslides • LiDAR • Segmentation • Characterisation • Geomorphometry

Introduction

Since the availability of Light Detection and Ranging (LiDAR), shaded-relief, slope, surface roughness and contour maps, and other derivatives have regained popularity for landslide inventory mapping, especially in forested areas (Schulz 2004; Van Den Eeckhaut et al. 2007, 2011).

Many studies have used expert-based analysis of LiDAR derivatives to identify landslides, while only few studies have attempted to develop computer-aided methods for extracting landslides from LiDAR data (McKean and Roering 2004; Booth et al. 2009). Promising results were obtained with

M. Van Den Eeckhaut (✉) • J. Hervás
Institute for Environment and Sustainability, Joint Research Centre (JRC), European Commission, 21027 Ispra, Italy
e-mail: miet.van-den-eeckhaut@jrc.ec.europa.eu

N. Kerle
Faculty of Geo-Information Science and Earth Observation, University of Twente, Enschede, The Netherlands

R. Supper
Geological Survey of Austria, Vienna, Austria

C. Margottini et al. (eds.), *Landslide Science and Practice*, Vol. 1,
DOI 10.1007/978-3-642-31325-7_13,

Table 1 Maps used in the Flemish Ardennes

Map	Additional information
Image layer (2 × 2 m resolution)	
DTM (m)	
Slope gradient (%)	
Plan- and profile curvature ()	
Edge_slope	Map obtained through edge detection (pixel min/max filter in eCognition) on Slope gradient map
Edge_slopecl	Expert-based classification of Edge_slope map
Dif_DTM_DTMki (m) with i = 15, 25, 50, 75	Difference between original DTM and DTMki, where DTMki is a raster map where each grid cell represents the mean value of a moving window with kernel size ki with i = 15, 25, 50, 75 (best result was obtained with i = 50)
Thematic layer (vector map)	
River	Derived from the DTM using the hydrology toolbox in ArcGIS

surface roughness parameters. So far, all these automated attempts have been carried out in a pixel-based analysis. However, with high resolution topographical data such as LiDAR, object-based or object-oriented analysis (OOA) might provide better results. OOA rests upon two inter-related methodological steps: (1) segmentation or regionalization of pixels, if necessary on different scales, into meaningful, homogeneous objects that reduce the noise inherent in pixel-based analysis, and that facilitate a multi-scale analysis (Blaschke 2010); and (2) rule-based classification incorporating spectral, textural, morphometric and contextual landslide features. It is clear that the quality of the segmentation largely controls the classification.

OOA has gained increased attention for (semi-) automated landslide identification from passive optical airborne and satellite sensor data (Barlow et al. 2003; Martha et al. 2010; Stumpf and Kerle 2011; Lu et al. 2011). These studies have proven the potential for creation of inventories of recent landslides of different types. However, until now Digital Terrain Models (DTMs) have only been used in the second step, the classification. The identification of old vegetated landslides, not detectable from passive optical images, has not been investigated so far. Van Asselen and Seijmonsbergen (2006) used LiDAR derivatives in an OOA for semi-automated geomorphological mapping. Their classification included slopes with mass movement. They did not focus on individual landslides as separation of individual landslides was considered difficult. Nevertheless, the objective of this study is to test OOA for landslide inventory mapping using only LiDAR data for both the segmentation and classification steps. As such we enter in the field of geomorphometry. More specifically, we will exploit the profound morphologic manifestation of old, densely vegetated landslides to semi-automatically map their extent using LiDAR derivatives, and we will outline the pros and cons of the methodology. We focus on two study areas: the Flemish Ardennes (Belgium) and Vorarlberg (Austria).

Materials and Methods

Data

The Flemish Ardennes is a hilly region characterised by loose tertiary lithology (alternation of clays and more sandy lithology) affected by more than 200 landslides (Van Den Eeckhaut et al. 2011). We refer to Van Den Eeckhaut et al. (2007) for a detailed description of the LiDAR data used for this region (AGIV 2005).

For Vorarlberg, an Alpine region with bedrock outcrops, we use more detailed LiDAR data provided by VoGIS (Rieger 2005). From the LiDAR point data, available in .txt format for the Flemish Ardennes and in ASCII format for Vorarlberg, 2 m resolution DTMs were created and after low pass filtering (kernel size 3) different LiDAR-derivatives were produced. The maps evaluated in this study (Table 1) are focussing on the lower order derivatives, which the human brain also uses for delineating landslide boundaries and classifying landslide parts (Minar and Evans 2008). The OOA was carried out in eCognition Developer 8.

Conceptualization of Landslides and Translation to OOA

The ultimate benchmark of OOA is human perception (Lang 2008). It has been widely recognized that compared to grid cells, objects are closer to human perception and patterns better represent real landscapes, if the scale is appropriate (Goodchild et al. 2007; Drăguţ et al. 2011). Our visual sense of any kind of object is a common experience, yet not always easy to communicate and even more difficult to translate into rule sets. Hence, (semi-)automated classification of landslides, almost always represents an attempt to replicate subjective landslide recognition (e.g. Martha et al. 2010). Stumpf and Kerle (2011) provide an overview

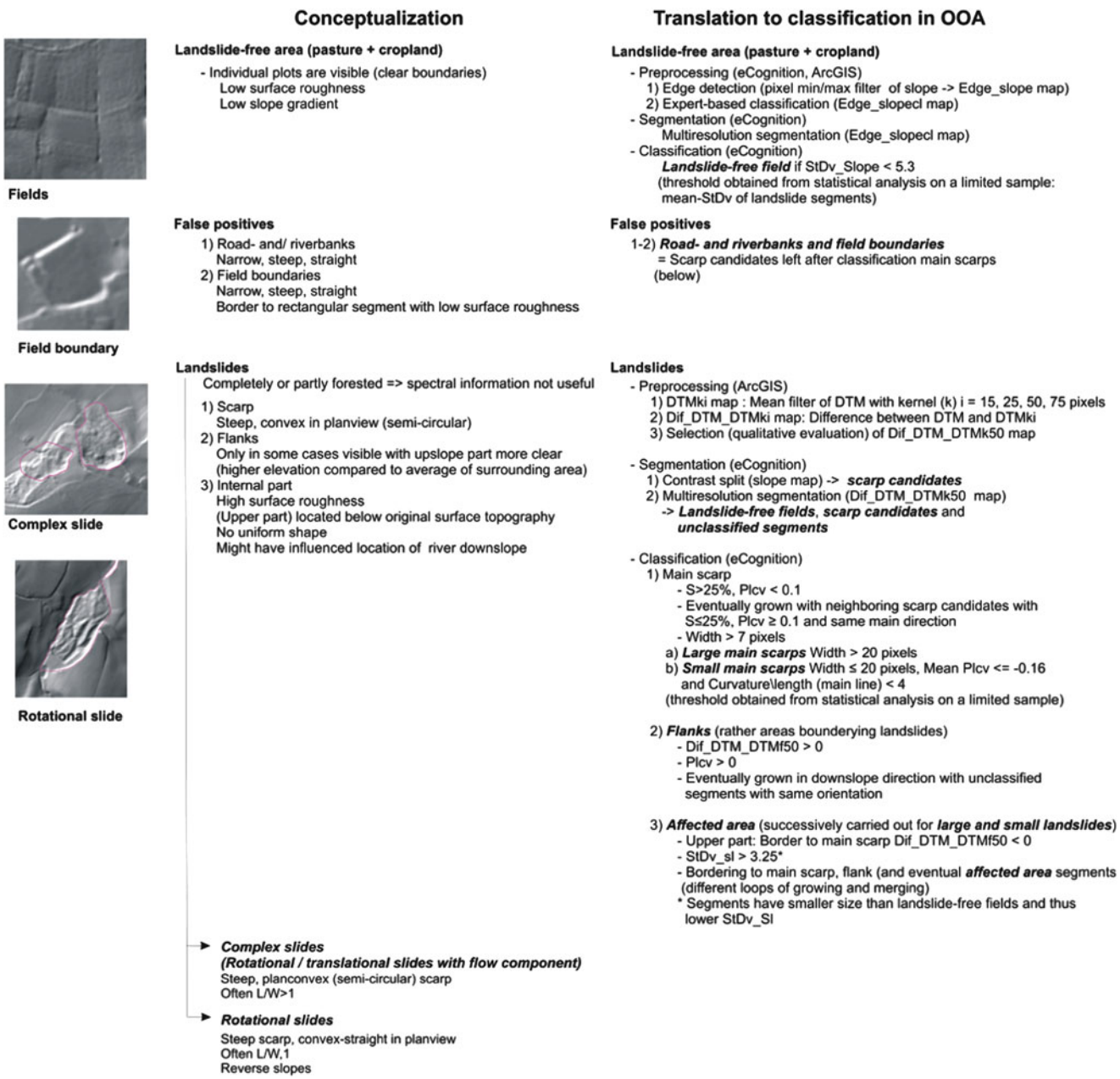

Fig. 1 Human conceptualisation of landslides and translation to object oriented analysis (*S*: slope gradient, *StDv_Slope*: standard deviation of slope gradient; *Plcv*: plan curvature)

of image object features previously used in OOA-based landslide inventory studies. Most of these features are not solely characteristic for landslides, and many are related to passive optical images (i.e. spectral information) making them not very useful in a LiDAR oriented approach where the focus should be put on identification of geomorphometric features. Figure 1 contains the conceptualisation of landslides typically found in the Flemish Ardennes, including old deep-seated rotational/translational slides with a flow characteristic (i.e. complex slides) and rotational slides. The figure also shows the conceptualisation of landslide-free terrain (mainly cropland and pastures) and possible false positive landslides (road-and riverbanks and field borders). The ultimate objective is to find a classification rule set based on the listed characteristics.

Translation of the landslide concept in eCognition starts with segmentation. Multiresolution segmentation was used in combination with Contrast Split segmentation (Fig. 1). The scale factor is the most important factor influencing the segmentation (Drăguţ et al. 2010). Although a relatively high number of studies have focussed on the influence of scale/resolution in terrain analysis, attempts to produce strategies for more objective selection of optimal scales are limited. Only recently several procedures for objective

selection of appropriate scales for multiresolution segmentation have been suggested (Martha et al. 2011; Stumpf and Kerle 2011). For this first analysis we used the estimation of scale parameter tool (ESP; Drăguţ et al. 2010).

For the study area in the Flemish Ardennes, the segmentation and classification procedure was calibrated for a 10 km^2 test area. It was then applied to the 50 km^2 area surrounding the test area (Fig. 2a). For the test and validation area, the existing landslide inventory map obtained through visual inspection of LiDAR derivative maps and field surveys (Van Den Eeckhaut et al. 2007) contains 4 and 14 rotational slides, 10 and 16 complex slides, 4 and 6 possible slides (less clear geomorphic manifestation) and 2 and 15 shallow slides, respectively. The latter are not taken into account in this study.

Results

Landslide Identification

Figure 1 shows the procedure followed for segmentation and classification. First, landslide-free agricultural fields were extracted. The segmentation procedure for this included detection of edges on the slope map and subsequent multiresolution segmentation using the resulting map (Edge_slopecl). Then, a sample of landslide-free field segments and landslide-affected segments was analysed and segments with a standard deviation of slope gradient below 5.3 were found to be landslide-free fields.

For extraction of landslides, the most distinct landslide characteristics, the main scarps, were extracted first, followed by the flanks and finally the landslide-affected area. Contrast Split segmentation of the slope map was carried out to separate steep (classified scarp candidates) from flatter terrain. The flatter terrain in this map was subsequently split with multiresolution segmentation of the Dif_DTM_DTMk50 map (Table 1) and the river map (Fig. 2a).

Main scarp segments were extracted from scarp candidates using their concave planform. As individual scarps could consist of several segments a growing procedure was subsequently used. Based on their width, large and small main scarp segments were separated, because during the calibration procedure more false positives were obtained for smaller main scarps.

Compared to main scarps, the morphologic manifestation of flanks is much less clear. No appropriate procedure has been found for segmentation of flank candidates yet, and thus the focus was not put on landslide flanks itself but on segments bordering the sides of the landslides. Especially for the upper part of the landslide, these segments are located above the surrounding segments (i.e. have mean

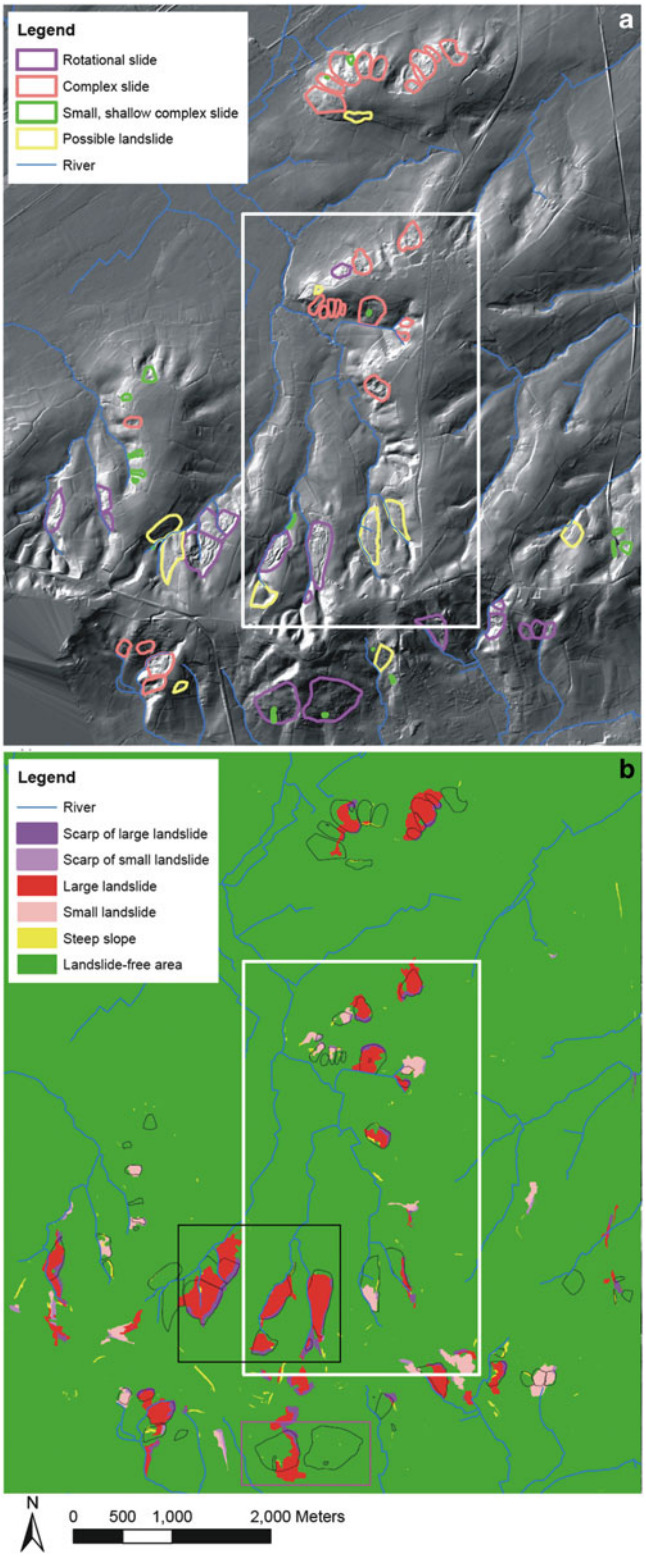

Fig. 2 Test (*white rectangle*) and validation area in the Flemish Ardennes: (**a**) The shaded relief map (LiDAR data © AGIV) is overlaid with the expert-based landslide inventory map created by Van Den Eeckhaut et al. (2007); (**b**) Preliminary landslide inventory obtained with OOA. *Black and purple rectangle* represent correctly identified and missed landslides, respectively

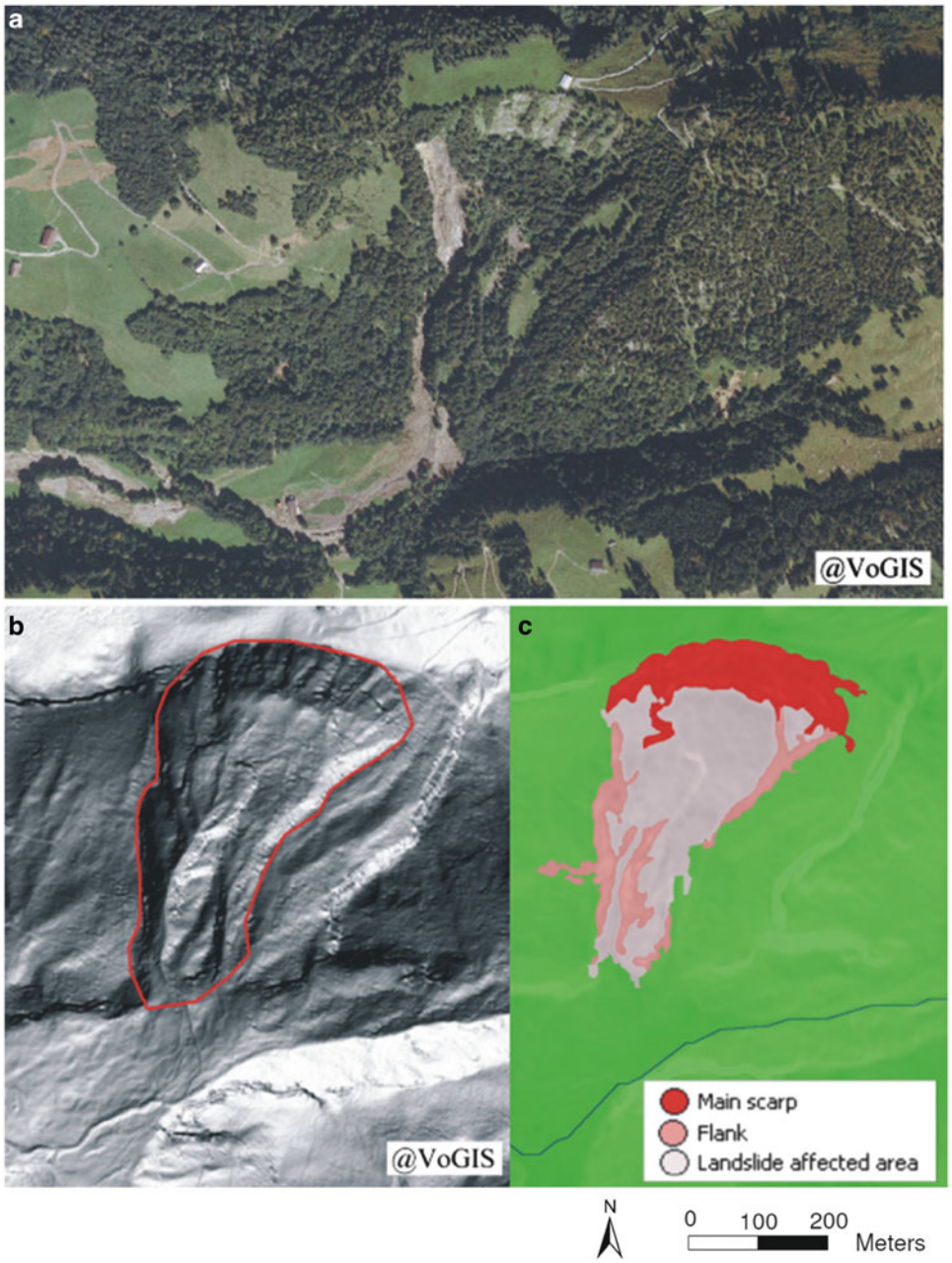

Fig. 3 Landslide under vegetation in Vorarlberg: (**a**) Orthophoto, (**b**) LiDAR-derived hillshade map; (**c**) preliminary result of segmentation and classification of the landslide (LiDAR data @ VoGIS)

Dif_DTM_DTMk50 > 0). The classification of the affected area started from the main scarp (first for the large and subsequently for the small) in downslope direction. Finally, the unclassified segments were classified as landslide-free field. The results obtained are shown Fig. 2b.

Accuracy Assessment

Accuracy assessment of geometric analysis is difficult to perform. First, there is no "completely perfect landslide inventory map" to compare the results against, as landslide inventory maps created from LiDAR analysis by different experts result in inventory maps with considerable differences (Van Den Eeckhaut et al. 2007). Second, currently there is no standard evaluation method for the assessment of the quality of image segmentation, let alone for multiresolution segmentation (Drăguţ et al. 2011).

A first accuracy assessment can be carried out by comparing the landslide inventory obtained with OOA (Fig. 2b) with the expert-based inventory (Fig. 2a). No difference in accuracy was found for the calibration and validation area. The rotational slides in the central south of the study area (i.e. black rectangle) are for example in agreement with the expert-

based inventory. The two large complex slides in the south (i.e. purple rectangle), however, are not identified with OOA. Their surface morphology is probably too subdued and affected by anthropogenic interventions (construction of houses and roads in the lower deforested part of the landslides).

The extent of about 70 % of the landslides was correctly identified with little differences between the accuracy obtained for complex and rotational slides. These results are in the same order as the results obtained by Martha et al. (2010). False negatives (unidentified landslides) are always landslides for which the main scarp was not correctly identified. In most cases the main scarps were initially identified as scarp candidates though later omitted because of a plan convex morphology. The observation that these false negatives generally have smaller main scarps supports the idea of distinguishing between large and small main scarps.

The OOA landslide inventory contains also about ten misclassified zones (group of segments incorrectly classified as main scarp and landslide). These are either steep valley heads (where some slope failure might not be excluded) or zones where a road bank or earthen bank bordering a field was misclassified as a main scarp and subsequently grown into a landslide. Generally, this last group of false positives has an irregular form.

Discussion

For (semi-)automatic mapping of densely vegetated landslides, an alternative to passive optical sensors has to be found for production of landslide inventory maps. Using LiDAR derivatives in an OOA we obtain similar accuracy results (i.e. approximately 70 %) compared to previous studies using OOA and passive optical remote sensing data (e.g. Martha et al. 2010), and thus it is worthwhile to further exploit the possibilities of OOA with LiDAR data.

In soil covered areas such as Flanders, landslides are generally characterized by a much higher surface roughness compared to the surrounding landslide-free areas, and therefore good first results were obtained with slope gradient and surface roughness (standard deviation of slope gradient) maps. The downslope part of old landslides, like those studied here, often has a poor geomorphometric signature. However, this problem has been reported for expert-based landslide inventory mapping to (e.g. Schulz 2004). For delineation of landslide boundaries also several edge detection procedures have been tested, but so far without great success.

In more mountainous areas, such as our second study site in Vorarlberg (Fig. 3), it is more difficult to distinguish landslides from non-landslide areas, because stable bed rock outcrops around landslides also have high topographic roughness. Additionally, the number of false positive main scarps is higher due to the presence of steep cliffs. As in the Flemish Ardennes also in Vorarlberg many landslides have flanks with a subdued morphologic signature. In some cases an internal drainage system has developed (Fig. 3), which further complicates the landslide classification process. Overall, compared to the case-study in Flanders transferability is more difficult. A rule set calibrated for one or two landslides does not work for many other landslides.

Some differences between the use of passive optical remote sensing data and active optical remote sensing data such as LiDAR were observed. The most important one is that when using passive optical remote sensing data, fresh landslides generally consist of one or a few segments only. However, landslides are geomorphologically complex and consist of different parts with different geomorphological characteristics. Hence, they are not represented by one single segment when obtained from LiDAR derivatives, and the aggregation from different segments into one final landslide segment is difficult.

Recent studies have focussed on objective classification of segments. Martha et al. (2011) used k-Means cluster analysis and Stumpf and Kerle (2011) random forests. It should be further investigated whether these approaches are also useful in the context of this study. Similar to Martha et al. (2010), so far thresholds were only obtained through basic statistical analysis of limited samples selected in the test area, but future research will focus on quantification of the process and transferability.

Conclusions

The results obtained show that OOA using LiDAR derivatives (such as slope gradient, curvature and difference in elevation) and edge detection allows recognition and characterization of profound morphologic properties of deep-seated landslides. Main scarp, landslide boundary, and landslide segments were successively classified. Overall about 70 % of the landslides of an expert-based inventory were also included in the object-oriented inventory. Unidentified landslides were misclassified, because they had a less profound or plan convex main scarp. Some plan concave road banks or river valley heads, on the other hand, were incorrectly classified as landslides.

Ongoing research mainly focuses on improvement of the segmentation and automating the classification procedure, both with the objective of increasing transferability.

Acknowledgments This study has been carried out in the framework of the EU-FP7 project SafeLand: Living with landslide risk in Europe: Assessment, effects of global change, and risk management strategies (Grant Agreement 226479; http://www.safeland-fp7.eu/). The authors thank VoGIS for providing the LiDAR data in Vorarlberg, and Prof. J. Poesen for his contribution to the creation of the expert-based landslide inventory of the Flemish Ardennes.

References

AGIV (2005) LIDAR hoogtepunten – brondata van Digitaal Hoogtemodel Vlaanderen (CD-ROM). MVG-LIN-AMINAL-afdeling Water en MVG-LIN-AWZ-afdeling Waterbouwkundig Laboratorium en Hydrologisch onderzoek, Brussel

Barlow J, Martin Y, Franklin SE (2003) Detecting translational landslide scars using segmentation of Landsat ETM + and DEM data in the northern Cascade Mountains, British Columbia. Can J Remote Sens 29(4):510–517

Blaschke T (2010) Object based image analysis for remote sensing. ISPRS J Photogramm Remote Sens 645:2–16

Booth AM, Roering JJ, Perron JT (2009) Automated landslide mapping using spectral analysis and high-resolution topographic data: Puget Sound lowlands, Washington, and Portland Hills, Oregon. Geomorphology 109:132–147

Drăguţ L, Tiede D, Levick S (2010) ESP: a tool to estimate scale parameters for multiresolution image segmentation of remotely sensed data. Int J Geogr Inf Sci 24:859–871

Drăguţ L, Eisank C, Strasser T (2011) Local variance for multi-scale analysis in geomorphometry. Geomorphology 130(3–4): 162–172

Goodchild MF, Yuan M, Cova TJ (2007) Towards a general theory of geographic representation in GIS. Int J Geogr Inf Sci 21:239–260

Lang S (2008) Object-based image analysis for remote sensing applications: modeling reality – dealing with complexity. In: Blaschke T, Lang S, Hay G (eds) Object-based image analysis spatial concepts for knowledge-driven remote sensing applications. Springer, Berlin/Heidelberg, pp 3–27

Lu P, Stumpf A, Kerle N, Casagli N (2011) Object-oriented change detection for landslide rapid mapping. IEEE Geosci Remote Sens Lett 8:701–705

Martha T, Kerle N, van Westen CJ, Kumar K (2010) Characterising spectral, spatial and morphometric properties of landslides for semi-automatic detection using object-oriented methods. Geomorphology 116(1–2):24–36

Martha T, Kerle N, van Westen CJ, Jetten V, Kumar K (2011) Segment optimisation and data-driven thresholding for knowledge-based landslide detection by object-based image analysis. Trans Geosci Remote Sens 49(12):4928–4943

McKean J, Roering JJ (2004) Objective landslide detection and surface morphology mapping using high-resolution airborne laser altimetry. Geomorphology 47:331–351

Minar J, Evans IS (2008) Elementary forms for land surface segmentation: the theoretical basis of terrain analysis and geomorphological mapping. Geomorphology 95:236–259

Rieger W (2005). Laserscanning-Befliegung Vorarlberg – Regionen Oberland und Walsertal sowie Erstellung vond Digitalen Gelandemodellen, Zl. LVA 603.02.04.04.09.08. Amt der Vorarlberger Landesregierung

Schulz WH (2004) Landslides mapped using LIDAR imagery, Seattle, Washington. U.S. Geological Survey Open-File Report 2004–1396, 11p, 1 plate

Stumpf A, Kerle K (2011) Object-oriented mapping of landslides using random forests. Remote Sens Environ 115(10):2564–2577

Van Asselen S, Seijmonsbergen AC (2006) Expert-driven semi-automated geomorphological mapping for a mountainous area using a laser DTM. Geomorphology 78:309–320

Van Den Eeckhaut M, Poesen J, Verstraeten G, Vanacker V, Nyssen J, Moeyersons J, Van Beek LPH, Vandekerckhove L (2007) The use of LIDAR-derived images for mapping old landslides under forest. Earth Surf Proc Landf 32:754–769

Van Den Eeckhaut M, Poesen J, Gullentops F, Vandekerckhove L, Hervás J (2011) Regional mapping and characterisation of old landslides in hilly regions using LiDAR-based imagery in Southern Flanders. Quat Res 75:721–733